

NUMERICAL ANALYSIS OF THE COUPLED POROELASTICITY USING THE FINITE ELEMENT METHOD

Francisco Ison da Silva Junior
ilson@fem.unicamp.br

Renato Pavanello
pava@fem.unicamp.br

Departamento de Mecânica Computacional
Faculdade de Engenharia Mecânica
Universidade Estadual de Campinas
Caixa Postal: 6122, CEP - 13083-970, Campinas-SP

Abstract. In this paper, a mixed displacement-pressure (u,p) formulation for poroelastic materials is used. The formulation is based on the Biot-Allard equations, written in terms of the structural phase displacement (u) and acoustic pressure in the pores (p). A Galerkin weak formulation is studied for the coupled equations of the acoustic-elastic wave propagation problem. The weak form has been discretized using the Finite Element Method. The numerical implementation of the present approach in a finite element code, using C++ language and OOP (Object Oriented Programming) techniques is discussed. Several analyzes in the frequency domain to acoustical and mechanical excitations in a single and multilayer poroelastic material are presented. The complexity of the model parameters difficult the physical interpretation of the results. To clarify the influence of some critical model parameters on the global poroelastic behavior, a systematic comparison about their influence in the dynamic response of the system was made. This paper also illustrates how this numerical model may help the optimization procedures of an acoustic insulation system.

Keywords. porous media, finite elements, absorption, Object Oriented Programming

1. Introduction

Poroelastic materials are frequently used in engineering applications such as: noise control of automobiles, acoustical insulation systems for aircrafts, environmental and domestic sound quality control, etc. In general, the poroelastic materials should be so light as possible and their damping and insulation properties must be designed for each specific case. A typical application is the design of the aircraft acoustical insulation system, where the poroelastic material properties, the layers configurations, the shape and the topology of the absorption system must be optimized. In Fig. (1), an acoustical insulation system of a jet is shown (Lamary et al, 2001). It can be noticed that the system is formed by several porous material layers.

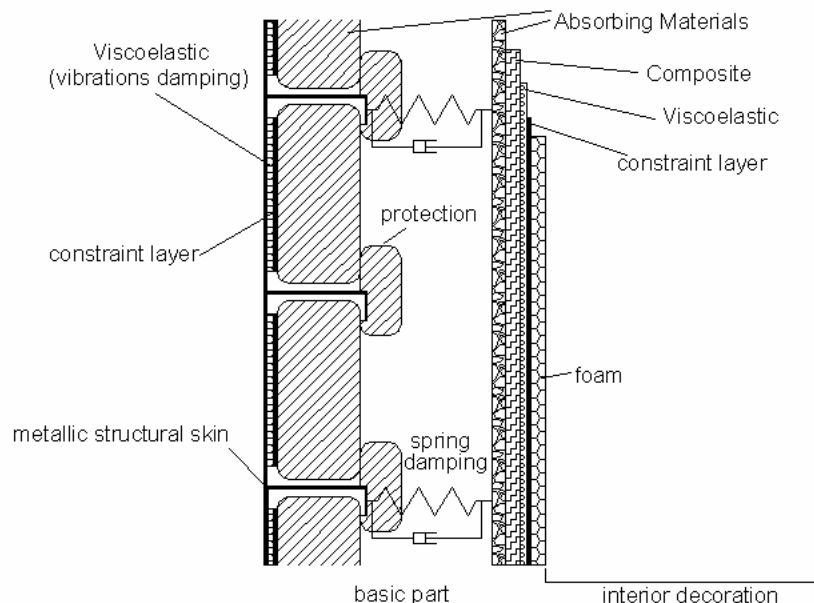


Figure 1. Acoustical insulating system of a business jet

A physical approach for understand and model the dynamic behavior of the poroelastic material, is based on the homogenization procedure of the solid and fluid phase properties (Zwikker and Kosten, 1949) and (Biot, 1956).

In a macroscopic level, the poroelastic medium can be represented by the continuum homogenized model showed in Fig. (2).

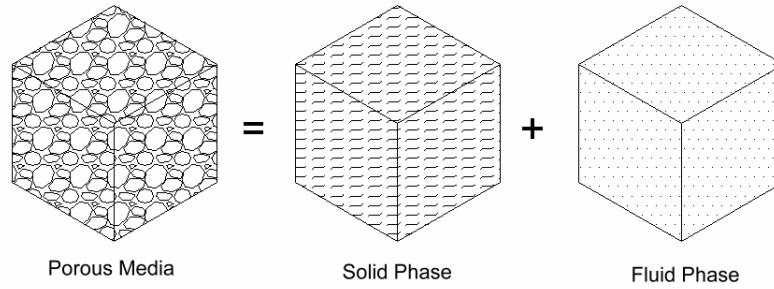


Figure 2. Phases of a porous material.

The homogenized medium could be represented using an elastic solid phase model coupled with an acoustical fluid phase model.

In this paper, a non symmetric formulation developed by (Atalla et al, 1996) is presented. The solid phase macroscopic displacement vector u_i and the interstitial fluid macroscopic pressure p are the state variables. The resultant coupled system is similar to the classical Fluid-Structure (u,p) system (Panneton and Atalla, 1997). A weak solution using a semi-discrete Finite Element model is adapted. Finally, a numerical analyze demonstrating the accuracy of the implementation approach is presented and a sensitivity analysis of the poroelastic parameters is shown.

2. Governing Field Equations

In this paper, the finite element formulation implemented is based on the partial differential equations formulated by (Depollier et al, 1988) and (Allard, 1993), using a non symmetric (u,p) formulation done by (Atalla et al, 1996).

The classic hypothesis for linear acoustic and elastic behavior are assumed (Allard, 1993). In this approach the wave propagation theory for the coupled medium is valid for low frequency range and fully saturated conditions. In this case, all dependent quantities represent small fluctuations around a static reference value and the poroelastic properties (porosity, tortuosity, etc) are continues in the domain.

The (u,p) formulation shows several advantages such as: low computational cost (four degrees of freedom per node) and compatibility with fluid-structure formulation. This formulation simplifies the assemblage process of the poroelastic systems, the imposition of its boundary conditions and its coupling with elastic and acoustic media.

Initially, the Biot-Allard displacement (u,U) formulation is briefly reviewed. This approach is basic for the development the (u,p) formulation terms.

2.1. The Biot-Allard (u,U) formulation

The model is based on the coupled poroelasticity equations, proposed initially by (Biot, 1956) and (Allard, 1993). Using the displacement formulation, the model is given by (Panneton and Atalla, 1998):

$$\sigma_{ij,j}^s = \rho_{11}\ddot{u}_i + \rho_{12}\ddot{U}_i + \tilde{b}(\dot{u}_i - \dot{U}_i), \quad (1)$$

$$\sigma_{ij,j}^f = \rho_{22}\ddot{U}_i + \rho_{12}\ddot{u}_i - \tilde{b}(\dot{u}_i - \dot{U}_i), \quad (2)$$

where σ_{ij}^s and σ_{ij}^f the stress tensor of solid and fluid phase, respectively.

The symbol $\tilde{}$ indicates that the associated physic property is a complex number and frequency dependent variable. In Eq. (1) and Eq. (2), u_i and U_i denote the vectors of average macroscopic displacements of the solid and fluid phases, respectively. These displacements are average values in the sense of the Biot theory, i.e., average volumetric displacements.

The densities ρ_{11} and ρ_{22} are mass coefficients that take into account the fact that the relative flow in the pores is not uniform. These factors are related to the mass density of the solid material phase, ρ_s , and the density of interstitial fluid, ρ_0 , in the following form:

$$\rho_{11} = (1-h)\rho_s - \rho_{12}, \quad (3)$$

$$\rho_{22} = h\rho_0 - \rho_{12}, \quad (4)$$

where h is the porosity of the material, defined as the ratio among the volume of voids (interstitial) and the total volume of the porous media. The density ρ_{12} quantifies the inertial interaction among the solid and fluid phases and is a function of the tortuosity α_∞ of the material (Bourbié and Coussy, 1987).

$$\rho_{12} = h\rho_0(\alpha_\infty - 1). \quad (5)$$

The structural damping associate with the solid phase can be included, using a classical structural damping model. Finally, \tilde{b} is a coefficient introduced by the viscous damping forces. This coefficient is frequency dependent and take in consideration the effects of the interactions between viscous fluid forces and elastic structural forces (Allard,1993).

$$\tilde{b} = h^2 \sigma \sqrt{1 + \frac{i\omega}{H}}, \quad (6)$$

where σ is the flow resistivity factor and H is the viscous characteristic frequency. σ and H are material proprieties measured by experimental procedures (Leclaire et al, 1996) and related by Eq. (7).

$$H = \frac{\sigma^2 \Lambda^2 h^2}{4\alpha_\infty^2 \eta \rho_0}, \quad (7)$$

where η represent the cinematic viscosity of the fluid and Λ is the network characteristic length of the porous material, introduced by (Johnson,1987).

2.2. The mixed displacement-pressure (u,p) formulation

A frequency domain dynamic (u,p) formulation has been implemented. It derives from Biot-Allard (u,U) formulation, Eq. (1) and Eq. (2). For harmonic motion the coupled system can be rewritten as (Panneton and Atalla, 1998):

$$\omega^2 \tilde{\rho}_{11} u_i + \omega^2 \tilde{\rho}_{12} U_i + \sigma_{ij,j}^s = 0, \quad (8)$$

$$\omega^2 \tilde{\rho}_{22} U_i + \omega^2 \tilde{\rho}_{12} u_i - hp_{,j} = 0, \quad (9)$$

where ω is the angular frequency. The effective densities for the poroelastic system, $\tilde{\rho}_{11}$, $\tilde{\rho}_{22}$ and $\tilde{\rho}_{12}$ are complex and frequency dependent variables (Panneton and Atalla, 1997):

$$\tilde{\rho}_{11} = \rho_{11} + \frac{\tilde{b}}{i\omega}, \quad (10)$$

$$\tilde{\rho}_{22} = \rho_{22} + \frac{\tilde{b}}{i\omega}, \quad (11)$$

$$\tilde{\rho}_{12} = \rho_{12} - \frac{\tilde{b}}{i\omega}. \quad (12)$$

Using Eq. (9), it is possible write the fluid displacement vector (U_i) in terms of the pressure gradient ($p_{,j}$) and solid displacement vector (u_i).

$$U_i = \frac{h}{\omega^2 \tilde{\rho}_{22}} p_{,j} - \frac{\tilde{\rho}_{12}}{\tilde{\rho}_{22}} u_i. \quad (13)$$

Substituting the Eq. (9) in Eq. (8), the solid phase equation transforms into:

$$\omega^2 \tilde{\rho} u_i + \frac{\tilde{\rho}_{12}}{\tilde{\rho}_{22}} p_{,j} + \sigma_{ij,j}^s = 0, \quad (14)$$

where $\tilde{\rho}$ is the complex effective density of the solid phase (Panneton and Atalla, 1997), defined as:

$$\tilde{\rho} = \tilde{\rho}_{11} - \frac{(\tilde{\rho}_{12})^2}{\tilde{\rho}_{22}}. \quad (15)$$

Note that the stress tensor of the solid phase, Eq. (14), is dependent of the fluid displacement vector (U_i), $\sigma_{ij,j}^s = \sigma_{ij,j}^s(u_i, U_i)$ (Biot, 1962) and (Bourbié and Coussy, 1987). The constitutive relations of the solid and fluid phase can be written by (Panneton and Atalla, 1998):

$$\sigma_{ij}^s(u_i, U_i) = \tilde{A}u_{i,i}\delta_{ij} + 2N\varepsilon_{ij}^s + \tilde{Q}U_{i,i}\delta_{ij}, \quad (16)$$

$$-hp\delta_{ij} = \tilde{R}U_{i,i}\delta_{ij} + \tilde{Q}u_{i,i}\delta_{ij}. \quad (17)$$

The terms \tilde{A} and N correspond to the Lamé coefficients for an elastic solid phase, \tilde{Q} is a coupling coefficient among the solid and fluid dilations and the stresses of the two phases, \tilde{R} can be interpreted as being the bulk modulus of the air occupying a fraction h of an unitary volume and δ_{ij} is the Kroneker delta.

Combining Eq. (16) with the Eq. (17) and knowing the relations of \tilde{A} , \tilde{Q} and \tilde{R} (Panneton and Atalla, 1998), the total stress tensor of the structural phase can be dismembered in two terms, one dependent of the solid phase and another of the fluid phase.

$$\sigma_{ij}^s(u_i, U_i) = \hat{\sigma}_{ij}^s(u_i) - h\frac{\tilde{Q}}{\tilde{R}}p\delta_{ij}, \quad (18)$$

where $\hat{\sigma}_{ij}^s(u_i)$ represent the elastic linear skeleton stress tensor in vacuum.

$$\hat{\sigma}_{ij}^s(u_i) = \left(K_b - \frac{2}{3}N \right) u_{i,i}\delta_{ij} + 2N\varepsilon_{ij}, \quad (19)$$

where K_b is the bulk modulus of the skeleton material in vacuum.

Substituting the Eq. (18) in Eq. (14), it is possible write the final relation of the coupled poroelasticity to the solid phase:

$$\hat{\sigma}_{ij,j}^s + \varpi^2\tilde{\rho}u_i + \tilde{\gamma}p_{,j} = 0, \quad (20)$$

where $\tilde{\gamma}$ is a new coupling term and defined as (Panneton and Atalla, 1998):

$$\tilde{\gamma} = h \left(\frac{\tilde{\rho}_{12}}{\tilde{\rho}_{22}} - \frac{\tilde{Q}}{\tilde{R}} \right). \quad (21)$$

and the simplified relations for \tilde{Q} and \tilde{R} can be written as (Panneton and Atalla, 1997):

$$\tilde{Q} = (1-h)\tilde{K}_f, \quad (22)$$

$$\tilde{R} = h\tilde{K}_f, \quad (23)$$

where \tilde{K}_f represents the bulk modulus of the air (Allard, 1993). It takes into account the effect of the fluid phase thermal interactions. This effect represent one energy loss and can be interpreted as one thermal damping. It is defined by (Dazel et al, 2002):

$$\tilde{K}_f = \frac{\theta P_0}{\theta - \left(\frac{(\theta-1)}{1 + (H'/2i\varpi)\sqrt{1+i\varpi/H'}} \right)}, \quad (24)$$

where H' is the thermal characteristic frequency given by:

$$H' = \frac{16\eta}{\text{Pr}\Lambda'^2 \rho_0}. \quad (25)$$

The variable θ is the ratio among the specific heats of the fluid, P_0 is the atmospheric pressure, Pr is the number of Prandtl of the fluid and Λ' is the thermal characteristic length (Champoux and Allard, 1991).

The Equation of the fluid phase is obtained substituting the divergence of the Eq. (13) in the Eq. (9):

$$\frac{h^2}{\tilde{\rho}_{22}} p_{,jj} + \varpi^2 \frac{h^2}{\tilde{R}} p + \varpi^2 \tilde{\gamma} u_{,i,i} = 0. \quad (26)$$

The Eq. (20) and Eq. (26) represent the mixed displacement-pressure (u,p) formulation for the coupled poroelasticity.

2.3. The weak form for the mixed formulation (u,p)

Using Galerkin's method in the Eq. (20) and Eq. (26), taking δu_i as the admissible virtual variation of the solid phase displacement vector (u_i) and δp as the admissible virtual variation of the fluid phase pressure field (p), one finds the weak form as:

$$\int_{\Omega} \hat{\sigma}_{ij}^s \cdot \delta u_{i,j} d\Omega - \varpi^2 \int_{\Omega} \tilde{\rho} u_i \cdot \delta u_i d\Omega - \int_{\Omega} \tilde{\gamma} p_{,j} \cdot \delta u_i d\Omega - \oint_{\Gamma} \hat{\sigma}_{ij}^s \cdot n_j \cdot \delta u_i d\Gamma = 0, \quad (27)$$

$$\int_{\Omega} \frac{h^2}{\tilde{\rho}_{22}} p_{,j} \cdot \delta p_{,j} d\Omega - \varpi^2 \int_{\Omega} \frac{h^2}{\tilde{R}} p \delta p d\Omega - \varpi^2 \int_{\Omega} \tilde{\gamma} \delta p_{,j} \cdot u_i d\Omega + \varpi^2 \oint_{\Gamma} \left(\tilde{\gamma} u^n - \frac{h^2}{\tilde{\rho}_{22} \varpi^2} \frac{\partial p}{\partial n} \right) \delta p d\Gamma = 0, \quad (28)$$

where Ω and Γ denote the poroelastic domain and its boundary, respectively. The vector n_j is the unitary normal vector of the boundary Γ , u^n is a scalar variable that represent the component of the structural displacement in the normal direction n_j and $\partial p / \partial n$ is the directional derivative of the fluid phase pressure.

For coupling porous material layers is not necessary calculate one interface matrix. The boundary integrals described in Eq. (27) and Eq. (28) account naturally poroelastic interfaces and enable the modeling poroelastic multilayer systems.

3. Finite Element Method for the poroelastic media

To solve the poroelastic problem expressed by weak formulation in the Eq. (27) and Eq. (28) some kind of approximation to the acoustic pressure and the structural displacement is needed. In the finite element method, this is achieved by expanding the unknown function in the following form:

$$u_i^e = [N^u] \cdot \{\bar{u}\}^e, \quad (29)$$

$$p^e = [N^p] \cdot \{\bar{p}\}^e, \quad (30)$$

where $[N^u]$ and $[N^p]$ are the matrices of the structural and fluid shape functions respectively, u_i^e is the nodal displacement vector of the solid phase, p^e is the nodal pressure vector of the fluid phase and e denote quantities relatives to an element.

Using the polynomial interpolation given by the Eq. (29) and Eq. (30) in the integral formulation, Eq. (27) and Eq. (28), the elementary matrices can be written as:

$$[K] = \int_{\Omega} [\ell]^t [N^u]^t \cdot [D] \cdot [\ell] [N^u] \cdot d\Omega, \quad (31)$$

$$[\tilde{M}] = \tilde{\rho} \int_{\Omega} [N^u]^t [N^u] d\Omega, \quad (32)$$

$$[\tilde{C}] = \tilde{\gamma} \int_{\Omega} [N^u]^t \nabla [N^p] d\Omega, \quad (33)$$

$$[\tilde{H}] = \frac{h^2}{\tilde{\rho}_{22}} \int_{\Omega} \nabla [N^p] \nabla [N^p] d\Omega, \quad (34)$$

$$[\tilde{Q}] = \frac{h^2}{\tilde{R}} \int_{\Omega} [N^p]^t [N^p] d\Omega, \quad (35)$$

where the matrices $[K]$ and $[\tilde{M}]$ are the equivalent stiffness and mass matrices for the solid phase, respectively. For the fluid phase, $[\tilde{H}]$ and $[\tilde{Q}]$ represent the equivalent kinetic and compression energy matrices, respectively, $[\ell]$ is the differential operator to elasticity problem and $[D]$ is the constitutive matrix.

Grouping Eq. (37) to Eq. (41) in a matrix form, the following coupled system is obtained:

$$\begin{pmatrix} [K] - \omega^2 [\tilde{M}] & -[\tilde{C}] \\ -\omega^2 [\tilde{C}]^t & [\tilde{H}] - \omega^2 [\tilde{Q}] \end{pmatrix} \begin{Bmatrix} \bar{u} \\ \bar{p} \end{Bmatrix} = \begin{Bmatrix} F^s \\ F^p \end{Bmatrix}. \quad (36)$$

4. Computational Implementation

The implementation uses no commercial tools and is done in the project Mefflab++, one program in development in the Computational Mechanic Department at Unicamp. The Mefflab++ have been addressed to set of classes with the responsibility of understanding, set up, and solve some poroelastic problem proposed.

The object oriented programming is formed by a group of objects, previously classified second their characteristics and similarities (attributes), which communicate through the sending of messages (methods). The methods act on the object data sending messages and executing tasks. This programming techniques offers, among other advantages, robustness and safety, producing programs with easy maintenance and continuous evolution.

The approach for poroelastic system problems using finite element showed in Eq. (36) has been implemented in C++. To solve the poroelastic dynamic problems, it is necessary calculate the frequency dependent the elementary matrices and assemblage the global matrices (equivalent mass and stiffness matrices) of the system. Solving the equation system, the operational mode for specific frequency is determined.

5. Numerical Results

To test the proposed implementation in the Mefflab++, three poroelastic problems have been implemented. The first one is a single column of a poroelastic material. The frequency response of the poroelastic columns, submitted to one mechanical excitation, is evaluated in the frequency range (0; 1500 Hz). One-dimensional linear elements has been used. The solutions are compared through two specific vibro-acoustics indicators: the mean square velocity of the solid phase, Eq. (37), and the mean square pressure of the fluid phase, Eq. (38).

$$\langle v^2 \rangle = \frac{\omega^2}{2\Omega_p} \bar{u}^t \cdot \int_{\Omega} [N^u]^t [N^u] d\Omega \cdot \bar{u}, \quad (37)$$

$$\langle p^2 \rangle = \frac{\rho_0 c_0^2}{2\Omega_p} \bar{p}^t \cdot \int_{\Omega} [N^p]^t [N^p] d\Omega \cdot \bar{p}, \quad (38)$$

where Ω_p is the porous volume and c_0 is the speed of the sound. The vibro-acoustic indicators in calculated using the following references: to mean square velocity $v_{ref} = 5 \cdot 10^{-8}$ m/s and to mean square pressure $p_{ref} = 2 \cdot 10^{-5}$ Pa. It is assumed a structure constrained at one end. The mechanical excitation consists in imposing a prescribed value of 10^{-8} m to the structural displacement at the node in the other end. The poroelastic material simulated was fiberglass, described in the Tab. (1).

Table 1. Physical properties and dimensions of the poroelastic materials in research

| | α_{∞} | ρ_s (kg/m ³) | σ (Ns/m ⁴) | h | N (kPa) | v | Λ (m) | Λ' (m) | Thickness (cm) |
|------------|-------------------|----------------------------------|----------------------------------|------|---------------|-----|----------------------|----------------------|-------------------|
| Fiberglass | 1.40 | 30 | 25000 | 0.95 | 21(1+i0.05) | 0 | $0.93 \cdot 10^{-4}$ | $0.93 \cdot 10^{-4}$ | 12 |
| Glass wool | 1.06 | 130 | 40000 | 0.94 | 2200(1+i0.1) | 0 | $0.56 \cdot 10^{-4}$ | $1.10 \cdot 10^{-4}$ | 10 |
| Blanket | 1.18 | 41 | 34000 | 0.98 | 110(1+i0.015) | 0.3 | $0.60 \cdot 10^{-4}$ | $0.87 \cdot 10^{-4}$ | 0.4 |
| Screen | 2.56 | 125 | $320 \cdot 10^4$ | 0.80 | 1000(1+i0.1) | 0.3 | $0.06 \cdot 10^{-4}$ | $0.24 \cdot 10^{-4}$ | 0.08 |
| Foam B | 2.52 | 31 | 87000 | 0.97 | 55(1+i0.055) | 0.3 | $0.37 \cdot 10^{-4}$ | $1.19 \cdot 10^{-4}$ | 0.5 |
| Foam C | 1.98 | 16 | 65000 | 0.99 | 18(1+i0.1) | 0.3 | $0.37 \cdot 10^{-4}$ | $1.21 \cdot 10^{-4}$ | 1.6 |

The results for velocity and pressure vibro-acoustic indicators are shown in Fig. (3) and Fig. (4), respectively:

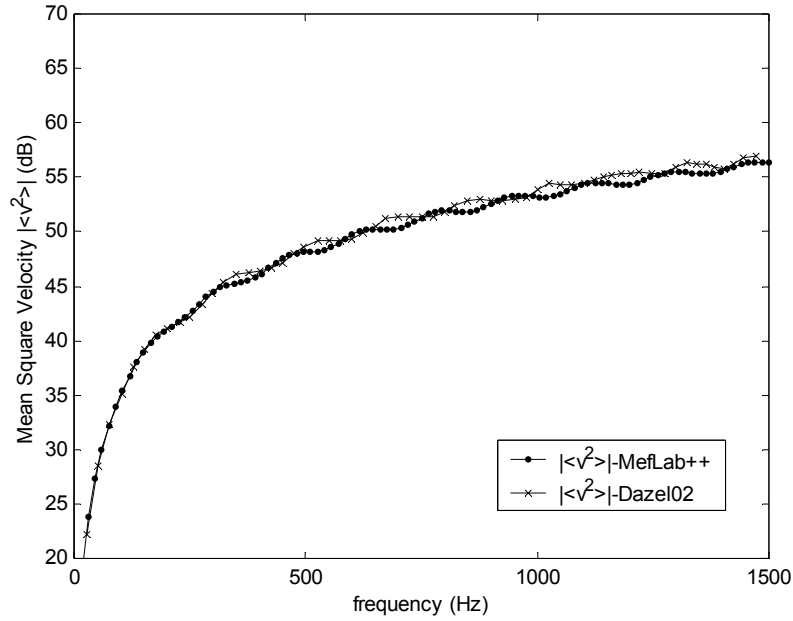


Figure 3. Mean square velocity for fiberglass with mechanical excitation

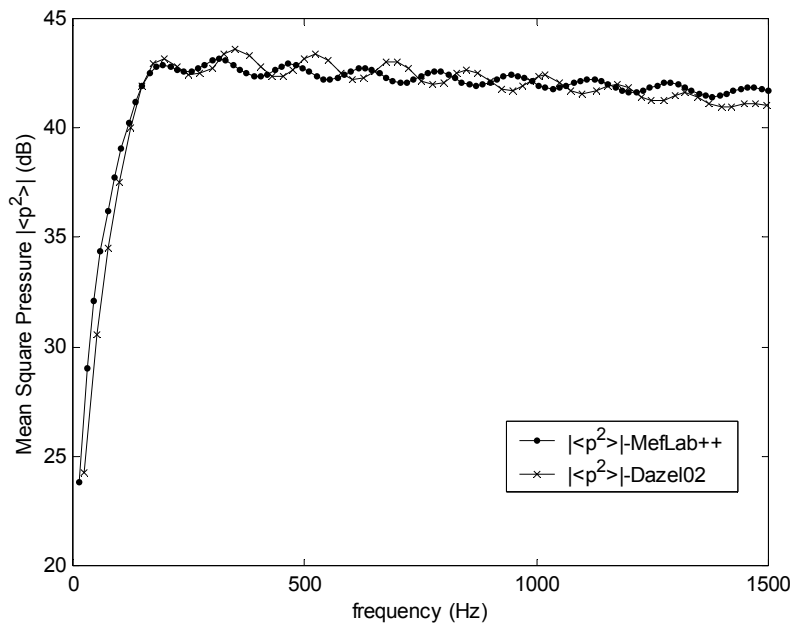


Figure 4. Mean square pressure for fiberglass with mechanical excitation

A good agreement is observed, showed in Fig. (3) and Fig. (4), when we compare with the results obtained in the formulation (u,p) in the work of (Dazel et all, 2002). Note that, in the terms of the average values, the dynamic responses are not in phase.

Another two tests show the values of the surface impedance of laterally infinite poroelastic material systems. Single and multilayer poroelastic systems are considered. The systems are bonded into a rigid impervious wall. A normal incident plane wave of unit amplitude excites the absorbing material.

In the single layer, the poroelastic material simulated is glass wool, described in the Tab. (1). For multilayer poroelastic problem, from the front face to rear face, it consist of a blanket, a screen, a foam B and a foam C, all of then described in the Tab. (1).

The configurations of the problems and the assumed boundary conditions are shown in Fig. (5):

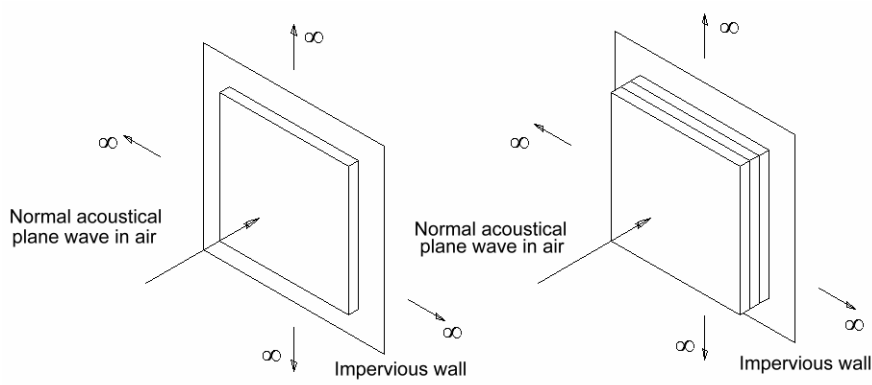


Figure 5. Single and Multilayer poroelastic materials in prescribing to the surface impedance

The values of surface impedance are obtained by pos-processing the poroelastic results. It is necessary calculate the fluid phase displacement vector (U_i), Eq. (13) and determine the surface impedance as:

$$Z_n = \frac{p}{\dot{w}} = \frac{1}{i\omega(hU^n + (1-h)u^n)} \quad (39)$$

These problems have been modeled by a linear mesh and the direction discretized has been of the thickness. The obtained impedance results are showed in Fig. (6) and Fig. (7).

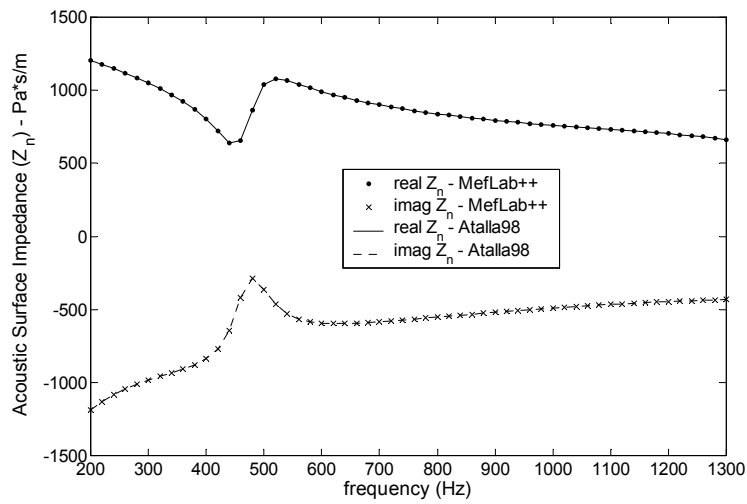


Figure 6. Surface Impedance, real and imaginary, for a single poroelastic material

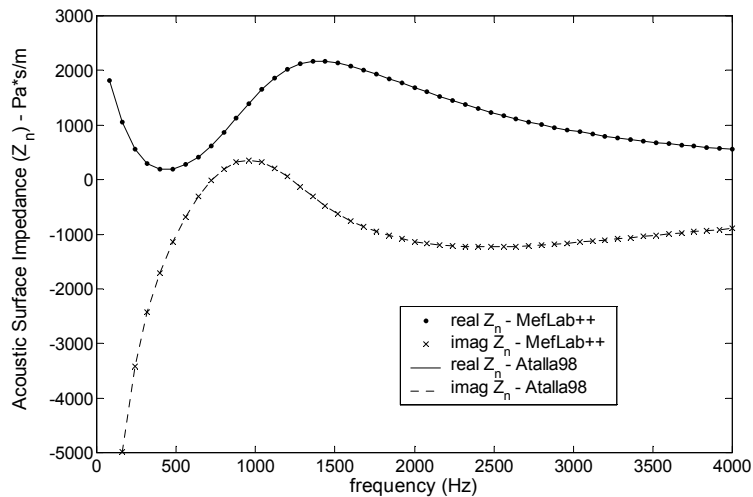


Figure 7. Surface Impedance, real and imaginary, for a multilayer poroelastic material

An excellent agreement of these results, showed in Fig. (6) and Fig. (7), is observed when compared with the results obtained in the work of (Panneton and Atalla, 1998).

5.1. Absorbing properties for a poroelastic multilayer system

In this section, several configurations of poroelastic multilayers are simulated. The initial system is similar that one analyzed in the previous section. The values of Foam B and Foam C thickness have been increase. The influence of thickness variation in the system absorbing properties are shown in Fig. (8) and Fig. (9).

With the surface impedance value, it is possible to determine the quantity of energy was absorbed by a poroelastic material in the surface of acoustical excitation. The absorbing coefficient is expressed by Eq. (40):

$$\alpha = 1 - \left| \frac{Z_n - \rho_0 c_0}{Z_n + \rho_0 c_0} \right|^2 \quad (40)$$

These type of graphics can be used in the insulation system design.

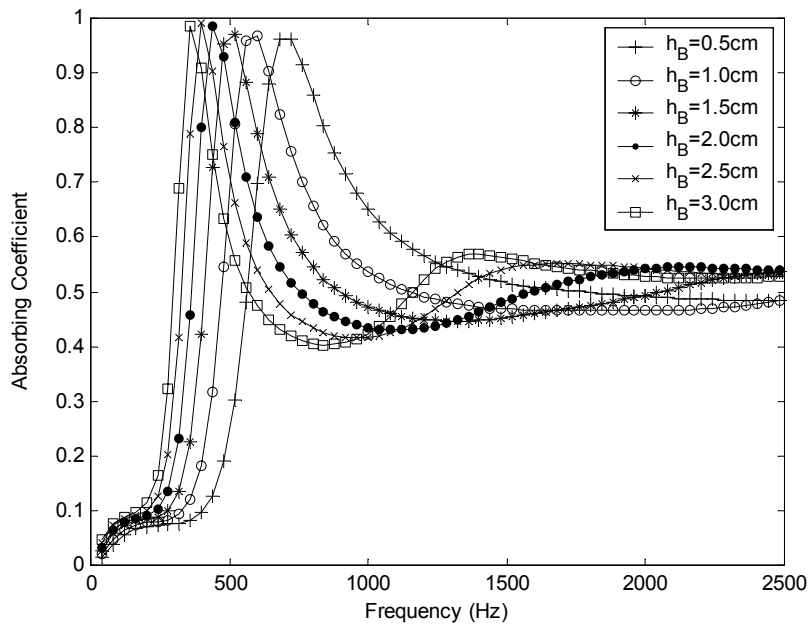


Figure 8. Absorbing coefficient for several simulations increasing the thickness of the poroelastic layer (Foam B)

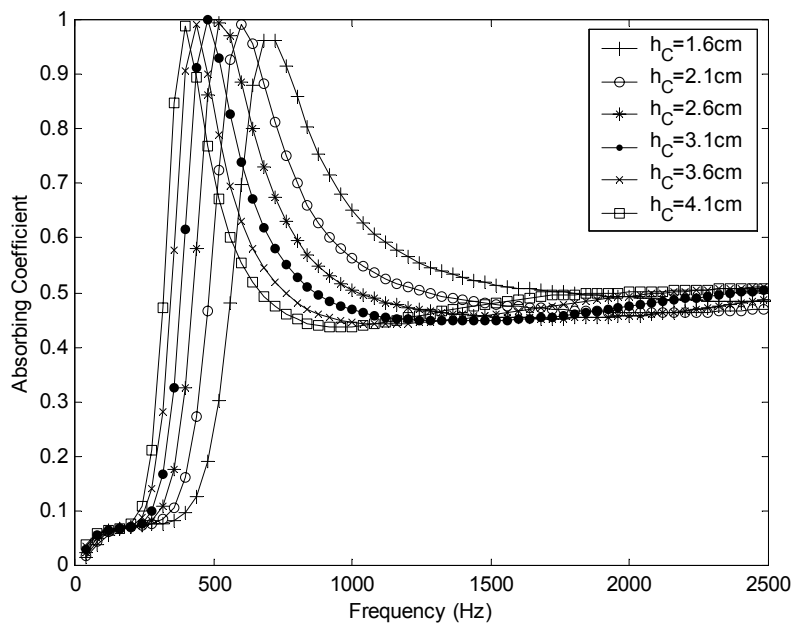


Figure 9. Absorbing coefficient for several simulations increasing the thickness of the poroelastic layer (Foam C)

The thickness is influent in the amplitude and in the system frequency values. For the case shown in the Fig (8), increasing the Foam B thickness, we can note one coupling to the first and second resonances of the system.

6. Conclusion

In this work, one implementation for the Biot-Allard (u,p) formulation has been done. The poroelastic equation system was approximated using the finite element method. An Object Oriented Programming technique has been used to implemented the poroelastic problem to the Meflab++ software.

The implementation of the mixed (u,p) formulation addressed to Meflab++ show good results for the proposed test problems. It was calculated the dynamic response to several poroelastic materials and configurations (single and multilayers materials). Vibro-acoustics indicators, surface impedance and absorbing coefficients are the parameters determined in one-dimensional analyses presented in this work.

It was possible to analyze the variation of the parameters and properties of the poroelastic materials in a simple insulation system. The absorbing coefficient results can be used as preliminary tool in the insulation system design and optimization.

7. Acknowledgement

I would like to thank CNPq, Capes and Fapesp for financial support for this work.

8. References

- Allard, J.F., 1993, "Propagation of Sound in Porous Media: Modeling Sound Materials", Elsevier, New York.
- Atalla N., Panneton R., Debergue P., Allard J.F., 1996, "A mixed displacement pressure formulation for Biot's poroelastic equations", 131st meeting of A.S.^a, Indianapolis.
- Biot M.A., 1956, "The theory of propagation of elastic waves in a fluid-saturated porous solid", Journal of Acoustical Society of America, 28:168-191.
- Biot M.A., 1962, "Generalized Theory of Acoustical Propagation in Porous Dissipative Media", Journal of Acoustical Society of America, 34:1254-1264.
- Champoux, Y. and Allard, J.-F. (1991). Dynamic tortuosity and bulk modulus in air-saturated porous media. Journal of Applied Physics, 70(4):1975-1979.
- D.L. Johnson, J. K. and Dashen, R., 1987, "Theory of dynamics permeability and tortuosity in fluid-saturated porous media", Journal of Fluid Mechanics, 176:379-402.
- Depollier, C., Allard, J. F., and Lauriks, W., 1988, "Biot theory and stress-strain equations in porous-absorbing materials", Journal of Acoustical Society of America, 84(6):2277-2279.
- Lamary, P., Tanneau, O., and Chevalier, Y., 2001. "Modelling poroelastic multilayered material for aircraft insulation", First European Forum - Materials and Products for Noise and Vibration Control in Machinery and Transportation, 1-10 pp.
- Leclaire, P., Kelders, L., and Lauriks, W. (1996), "Determination of the viscous and thermal characteristic lengths of plastic foams by ultrasonic measurements in helium an air", Journal of Applied Physics, 80(4):2009-2012.
- O. Dazel, F. Sgard, C.-H. L. and Atalla, N., 2002, "An extension of complex modes for the resolution of finite-element poroelastic problems", Journal of Sound and Vibration, 253(2):421-445.
- Panneton, R. and Atalla, N., 1996, "Numerical prediction of sound transmission through multilayer systems with isotropic poroelastic materials", Journal of Acoustical Society of America, 100:346-354.
- Panneton, R. and Atalla, N. 1997, "Low-frequency approximations for acoustic porous materials: Linearization of the poroelastic eigenvalue problem", Transactions of the CSME, 4:401-413.
- Panneton, R. and Atalla, N., 1998, "A mixed displacement-pressure formulation for poroelastic materials", Journal of Acoustical Society of America, 104(3):1444-1452.
- T. Bourbié, O. Coussy, B. Z., 1987, "Acoustics of Porous Media", Institut Français du Pétrolé Publications, Paris.
- Zwikker, C. and Kosten, C. W., 1949. "Sound Absorbing Materials", Elsevier Publishing Company.

9. Copyright Notice

The author is the only responsible for the printed material included in his paper.